PNAS
www.pnas.org

Supplementary Information for

Exceptionally high levels of lead pollution in the Balkans from the Early Bronze Age to the Industrial Revolution

Jack Longman, Daniel Veres, Walter Finsinger, Vasile Ersek

Jack Longman
Email: j.longman@soton.ac.uk

This PDF file includes:

Supplementary text
Figs. S1 to S7
Tables S1 to S2
Captions for databases S1 to S3
References for SI reference citations

Other supplementary materials for this manuscript include the following:

Datasets S1 to S3

www.pnas.org/cgi/doi/10.1073/pnas.1721546115

Supplementary Information Text

Subhead. Type or paste text here. This should be additional explanatory text such as an extended technical description of results, full details of mathematical models, extended lists of acknowledgments, etc.

Methods and Materials

Sampling

270 cm of sediment was collected via two overlapping and parallel cores extracted with a Russian peat corer. Each drive was 1m long, and the collected core was 8cm in diameter. The core was transferred to PVC tubes, wrapped and stored at 4°C prior to analysis. Between 270-255cm (7500 – 7000 BCE) the core is composed of reddish-brown silt, with coarse sand and gravel. Above is a gradual transition into olive-green silts up to 238cm depth (6400 BCE) prior to organic-rich dark brown coarse detrital gyttja. Finally, above 100cm (1500 BCE), the record is composed of fibrous sedge/Sphagnum-dominated peat.

Trace Metal Analysis

To allow the solid peat samples to be run via ICP-OES, total digestion was performed. Sampling for trace metal analysis was performed using plastic tools, and with subsamples taken from the inner portion of the core to ensure no contamination. Prior to all digestion, each section of peat was dried at 105^0C overnight before being homogenized using a pestle and mortar.

Digestion was performed using nitric acid (HNO_3), in combination with hydrochloric acid (HCl), in a ratio of 3:1; reverse aqua regia. To ensure total dissolution was achieved, hydrofluoric acid (HF) was added. Digestion was performed on roughly 0.2g of dried, crushed sample. Added to this was 12ml of reverse aqua regia (9ml of HNO_3 and 3ml of HCl) before addition of 1ml concentrated HF into a Teflon digestion vessel equipped with a vent for gas. Total dissolution was achieved using a microwave accelerated reaction system, with a 40 minute heating phase followed by a 20 minute cooling. Samples were then decanted into 50ml centrifuge vials, and diluted to 50ml with milli-Q deionized water.

9ml of sample was added to 1ml of 10ppm Yttrium Spex CertiPrep internal standard (producing a final solution containing 100ppm of the internal standard), dependent upon the elements being analyzed in that run. An internal standard is used to check for instrumental drift throughout a run. A number of blanks and 10 standards were also run. The two standards used are Montana 2711 soil and Peat Standard NIMT/UOE/FM001 (1), digested using the same method as the samples. Results (reference recoveries) are reported in Table S1. All Pb calculation data may be found in Supplementary dataset 1, whilst raw data (including SDs) may be found in Supplementary Dataset 2. Repeat data may be found in Supplementary Dataset 3.

Anthropogenic Component Extraction

Firstly, using the concentration of a conservative, lithogenic element (in this case zirconium (Zr), and the expected composition of the upper continental crust (UCC)(2), the lithogenic fraction was calculated (3):

$$Pb_{Lithogenic} = Zr_{Sample} \times (Pb_{UCC}/Zr_{UCC})$$

This value was subtracted from the overall Pb concentration of each sample to provide the likely anthropogenically-derived Pb fraction:

$$Pb_{Anthropogenic} = Pb_{Sample} - Pb_{Lithogenic}$$

Enrichment Factor

Utilizing Zr as the conservative element, the following calculation (4) may be made:

$$EF = \frac{Pb_{sample}}{Zr_{sample}} \Big/ \frac{Pb_{UCC}}{Zr_{UCC}}$$

Cumulative Anthropogenic, Atmospheric Pb

Using Pb_{Anthro} as calculated before, a graphical representation of the development of Pb deposition may be prepared. To perform this, Pb_{Anthro} in the entire core is summed, and the relative percentage of Pb_{Anthro} per sample is calculated. The CAAPb is simply a summation of each sample on top of all those which are below it.

Pb Accumulation Rate

The following equation is used to calculate Accumulation Rates:

$$PbAR = Pb_{sample} \times (\rho S_{sample})/\Delta t$$

Where Pb_{sample} is the total Pb concentration of the sample (ppm, or mg/kg); ρ is the bulk density (g cm^{-3}); S_{sample} the thickness of the sample slice (cm) and Δt is the time span of that slice (in years).

Changepoint analyses

It has been proposed (5) that changepoint modelling may be performed on multiple datasets from the same geochemical record, under the assumption of common changepoints between different datasets (6). However, at Crveni Potok the minerogenic nature of much of the peat record may render the use of mobile metal concentrations (Zn, Ni, Cu) to reconstruct pollution perhaps incorrect in places. Therefore, we relied on comparing changepoints obtained based on different statistical methods.

Changepoint analyses were performed with three different methods (Binary Segmentation (BS), Bayesian Change-Point analysis (BH), and breakpoints analysis (BP)) in order to show that the findings are not method-dependent. We performed changepoint analyses for the following datasets: Pb_{Anthro} concentration (Fig. 2F), Pb_{Anthro} accumulation rate (Fig. S4), and total Pb concentration (Fig. S5) to check for consistency of the results among the different Pb-quantification estimates.

The BS analysis for change points (7) is based on variations of the mean and variance and is one of the most widely used change-point search methods (8). We used it to compare change points in the measured PbAR record and in PbAR records obtained with random Pb concentration series (Figs. S5, S6) (9). The rationale is that because PbAR are obtained by multiplying the concentration values by the sediment-accumulation rates, variations in PbAR may strongly depend on variations of the depth-age model. Thus, if change points detected in random Pb records match change-points detected in the measured Pb records, such points may be spurious. As may be seen from our results, no such matching change points may be observed (Figs. S5, S6), indicating the variations in Pb are not artefacts of changing accumulation rate.

The BP method uses a dynamic programming algorithm (10) to identify optimal partitions with varying numbers of segments. The user can select the minimum segment length (*h*, here *h*=2), and the maximum number of breaks (m, here m=the maximum number allowed by *h*). For each possible number of breaks $k \leq m$, the BP method provides the optimal break-point locations by minimizing the within-segment sums of

squares. The R implementation of BP (11) selects the partition having the lowest BIC value.

The BH method uses a Markov-Chain-Monte-Carlo (MCMC) approximation of a Bayesian procedure (12). The method differs substantially from the BS and BP methods because it does not estimate the location of change points. Instead, it estimates the probability of a change point at each location, providing a more informative summary reflecting the degree of uncertainty in the change points.

All computations for the change-point analyses were performed under the R computing environment (13). Records were resampled using the pretreatment.full() function (available at https://github.com/wfinsinger/cpt-AR), which is a slightly modified version of the one available in the paleofire package (14), and gives the full output of the pretreatment function (15). The Binary Segmentation analysis for change points was performed using the 'changepoint' v2.2.2 package (8). The Bayesian analysis for change points (12) was performed using the 'bcp' package v 4.0.0 (16). The computation of breakpoints in regression relationships (11) was performed with the 'strucchange' v1.5-1 package (17).

Prior to performing the change-point analyses, we first linearly interpolated the datasets in order to fill sampling gaps. Thereafter, we resampled the raw datasets to a constant temporal resolution (here the median sampling resolution of 36 years sample^{-1}) to account for unequal sampling intervals resulting from variable sediment-accumulation rates.

Ombrotrophy

Initial surveys at Crveni Potok indicated no evidence of inflow from permanent streams (18), suggesting mineral input to the bog from the surrounding gentle slopes is very minimal, perhaps occurring only during periods of high rainfall. This was clear when describing the core, where no mineral matter was observable with the naked eye within the peat section, although some may be observed within the underlying gyttja. Geochemically, low strontium (Sr) concentrations (<20 ppm) have previously been used to assess the ombrotrophy of bogs (19, 20). The Sr concentration values measured at Crveni Potok are relatively low (15-35ppm, see Fig. S2) and suggest only minimal influences of runoff-derived Sr. The trends in erosion and minerogenic debris indicators (Zr, Sc, Ti as well as *Coenococcum* sclerotia, Fig. S3) further hint at episodic/occasional inputs of minerogenic matter. In keeping with this, close inspection of the uppermost 100cm of the record indicates *Sphagnum*-dominated peat, rendering this part of the record typical of a spruce-forest mire (20, 21). Hence, it is very likely that the Crveni Potok peat has never been truly ombrotrophic. Other sources of Sr may potentially include dust from the extensive Danube loess fields (22), or from the underlying limestone. Despite the apparent minerotrophic nature of Crveni Potok, this does not preclude its use for such paleopollution studies, with examples from Switzerland (23), and Spain (24), proving that metal concentrations reflect a coupled link to the atmospheric (particularly Pb, but also other metals) record even in such depositional environments.

Nevertheless, Sr concentrations are overall negligible when compared to other sites where regular influx of minerogenic debris from proximal slopes has been observed (25). Further elemental indicators of minerogenic input (Zr and Sc, Fig S3) are also much

lower than one would expect in a site influenced by regular runoff or flooding (25). Furthermore, there are very low correlations between Pb and any of these elements (Pb-Zr= -0.151, Pb-Sc= -0.166, Pb-Sr= -0.19) and so it is unlikely any possible proximal mineral influx is biasing the Pb record.

Regardless, all Pb data interpreted have been normalized to a conservative element (Zr) in order to disentangle the natural Pb lithogenic contribution to the reconstructed anthropogenic Pb record of Crveni Potok (Fig. 4).

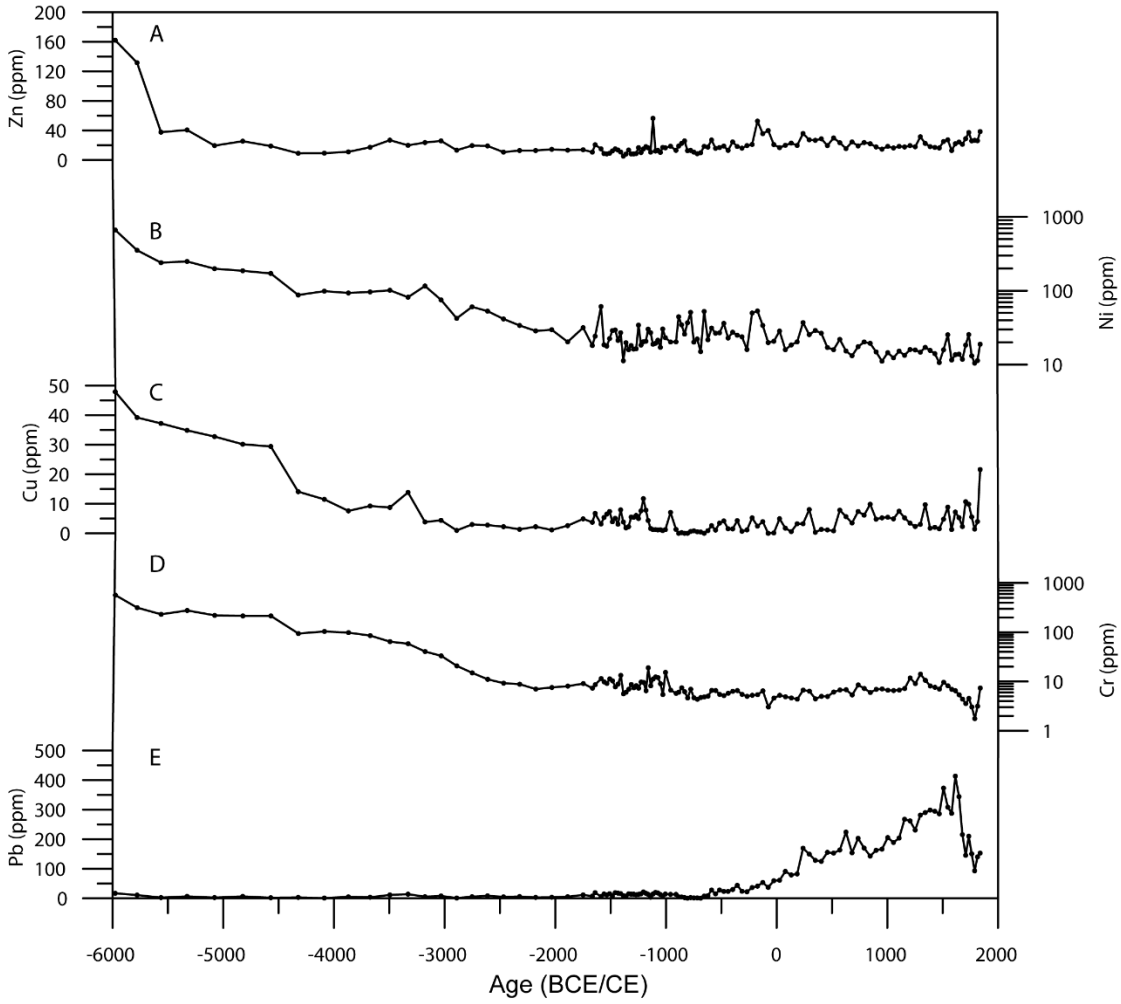

Fig. S1. Raw metallic elemental concentrations for Crveni Potok sediment sequence. Note logarithmic scale for Ni and Cr records.

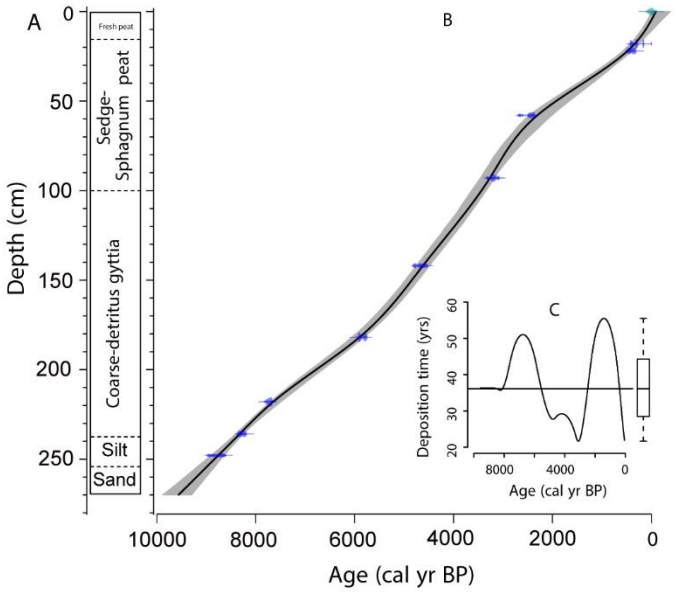

Fig. S2. A. A simplified lithological diagram of the core from Crveni Potok. B. The age model for the Crveni Potok sediment profile. C. Sample deposition times (years sample-1) plotted together with a boxplot indicating median (horizontal line) and the first and third quartiles (21)

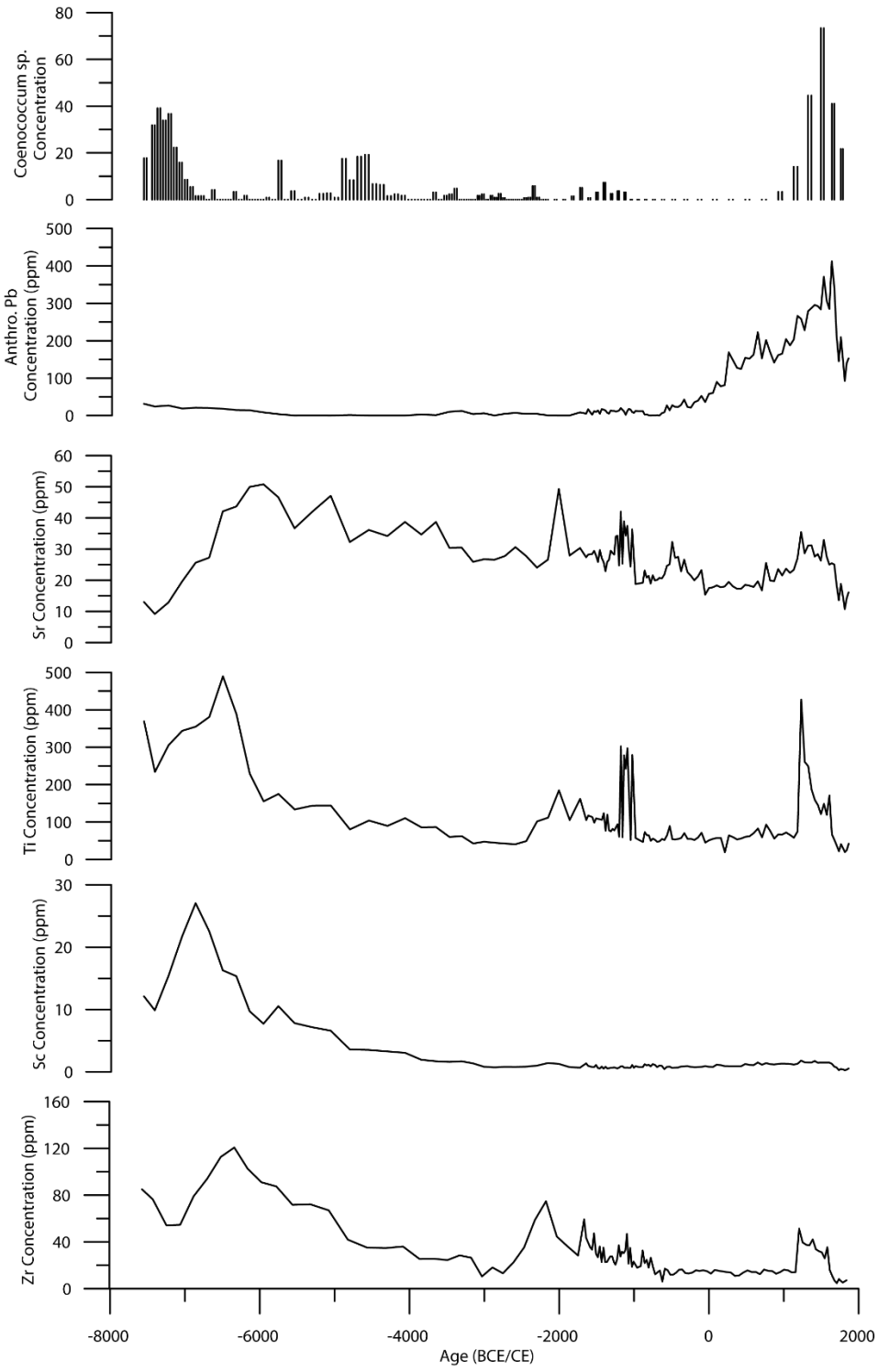

Fig. S3. Lithogenic proxies used to determine potential input of non-pollution related metals to Crveni Potok. A Coenococcum sp. (a fungi species generally related to soil erosion) concentrations. B Pb_{Anthro}. Panels C, D, E and F display lithogenic element concentrations; Sr, Ti, Sc and Zr, respectively.

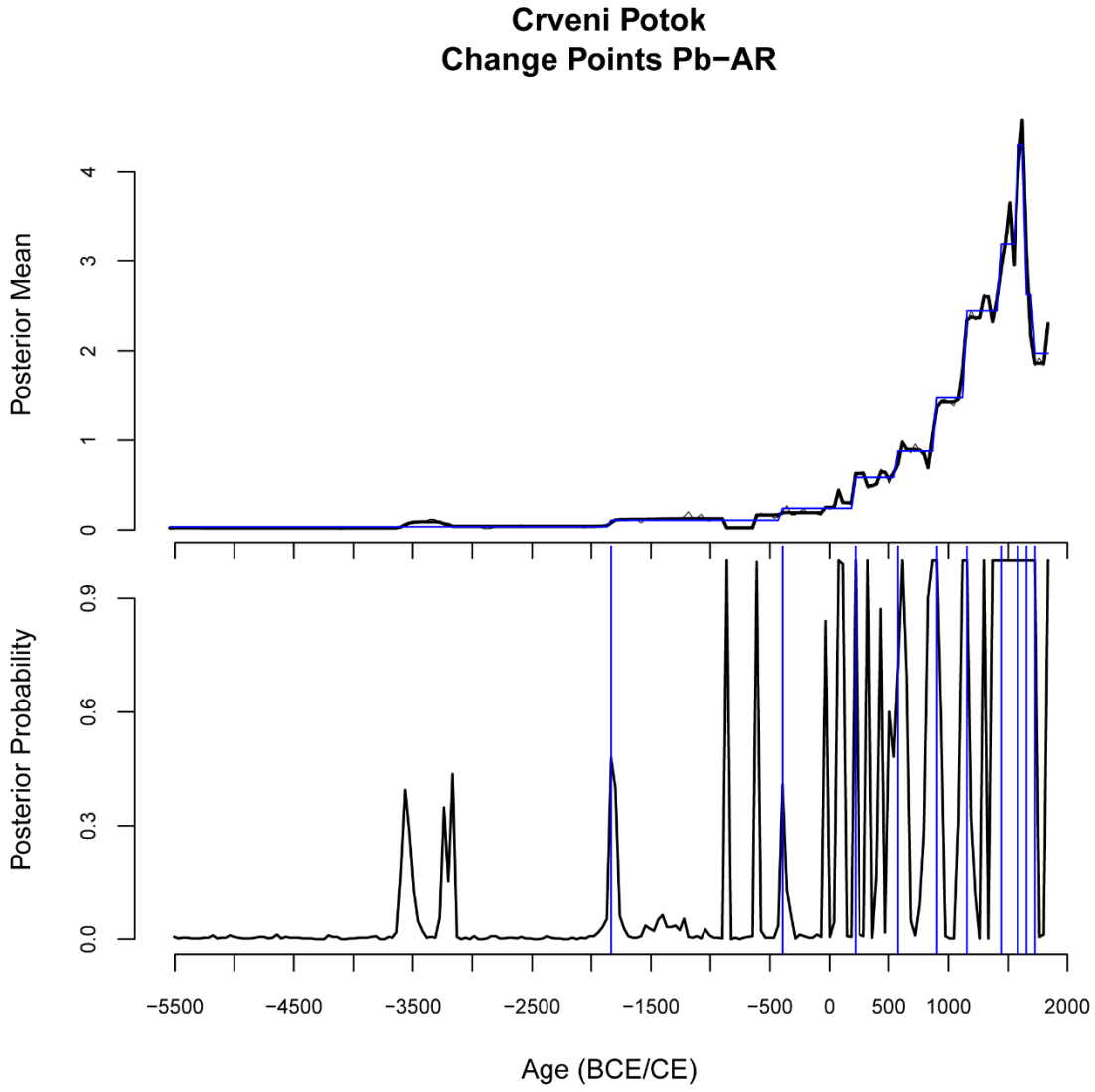

Fig. S4. BH and BP estimates of change points on the Pb_{Anthro} accumulation rate ($Pb_{Anthro}AR$) record. The black lines represents BH, the blue lines represent BP. In the lower plot, the black lines represent Barry and Hartigan's posterior probabilities of changes, and the blue vertical lines the change point locations of BP.

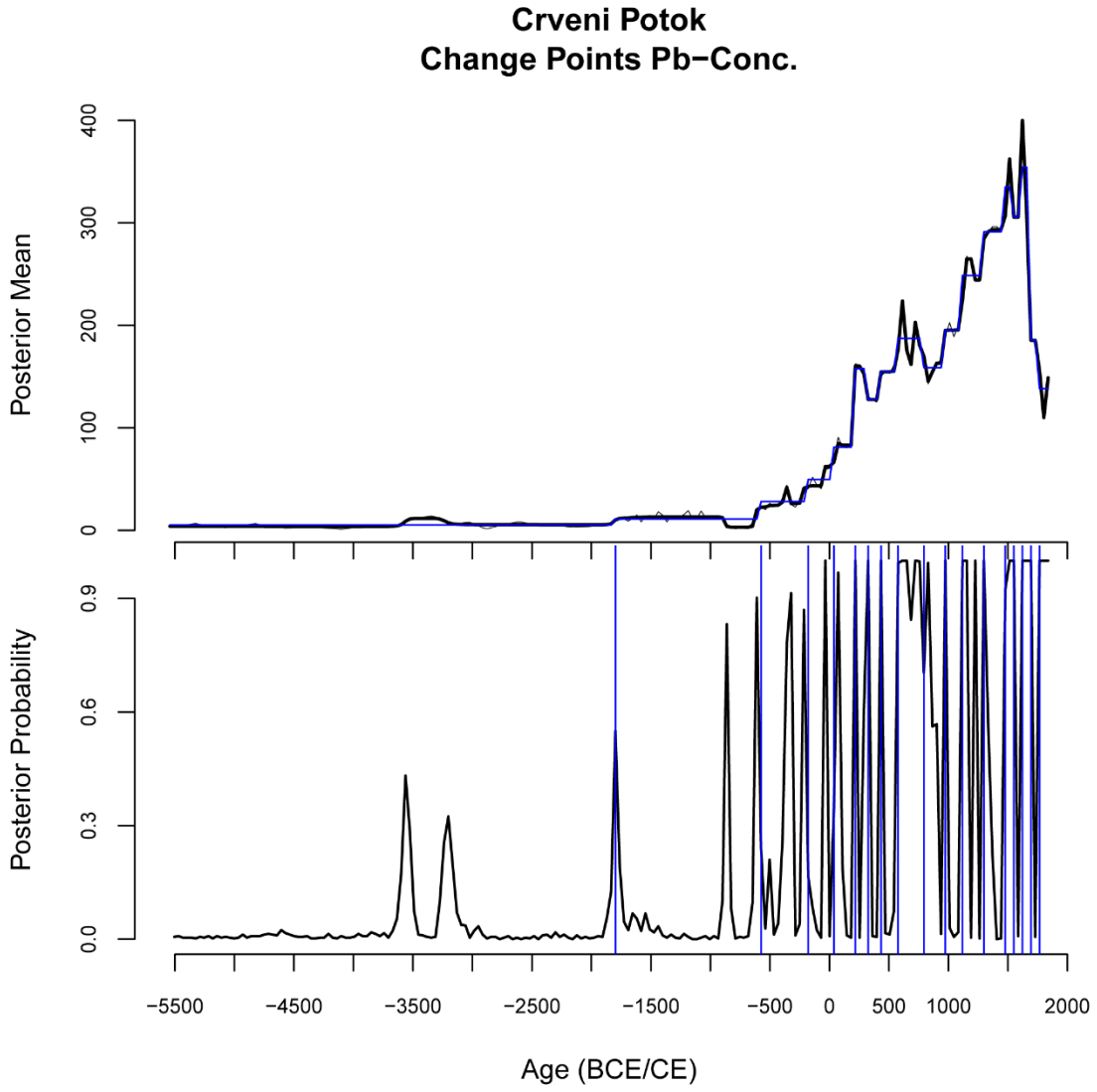

Fig. S5. BH and BP estimates of change points on the raw Pb concentration record. The black lines represents BH, the blue lines represent BP. In the lower plot, the black lines represent Barry and Hartigan's posterior probabilities of changes, and the blue vertical lines the change point locations of BP.

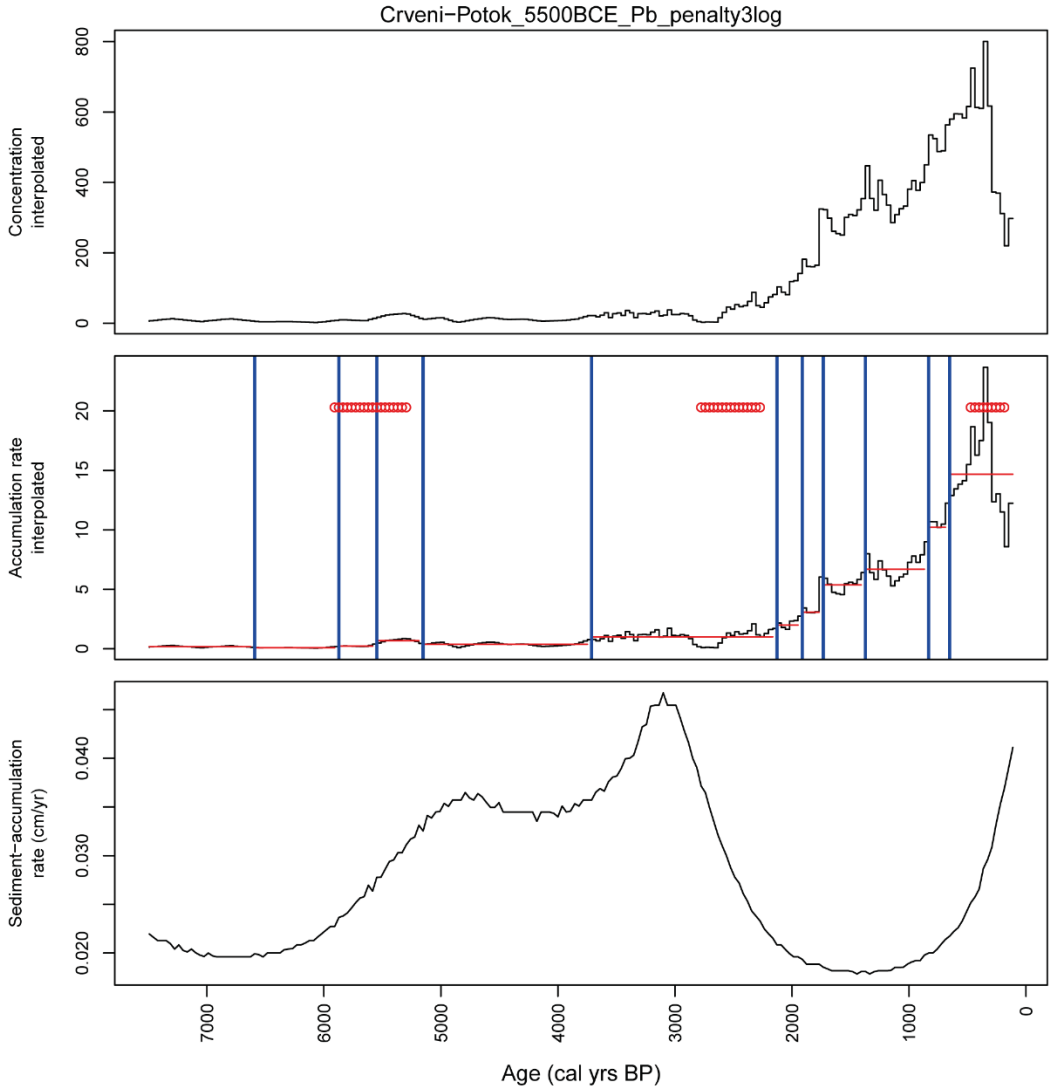

Fig. S6. Comparison between BS analysis for change-points and sediment-accumulation rates for the Pb_{Anthro} accumulation rate record of the Crveni Potok sediment sequence. Black lines in top and middle panels: interpolated Pb_{Anthro} record; vertical blue lines: change points in the measured Pb series. Change points in Pb records based on random Pb-concentration records appear as empty red circles in the middle panel under these low sensitivity test conditions (penalty = 3*log(n) = 15.98, where n is the number of datapoints).

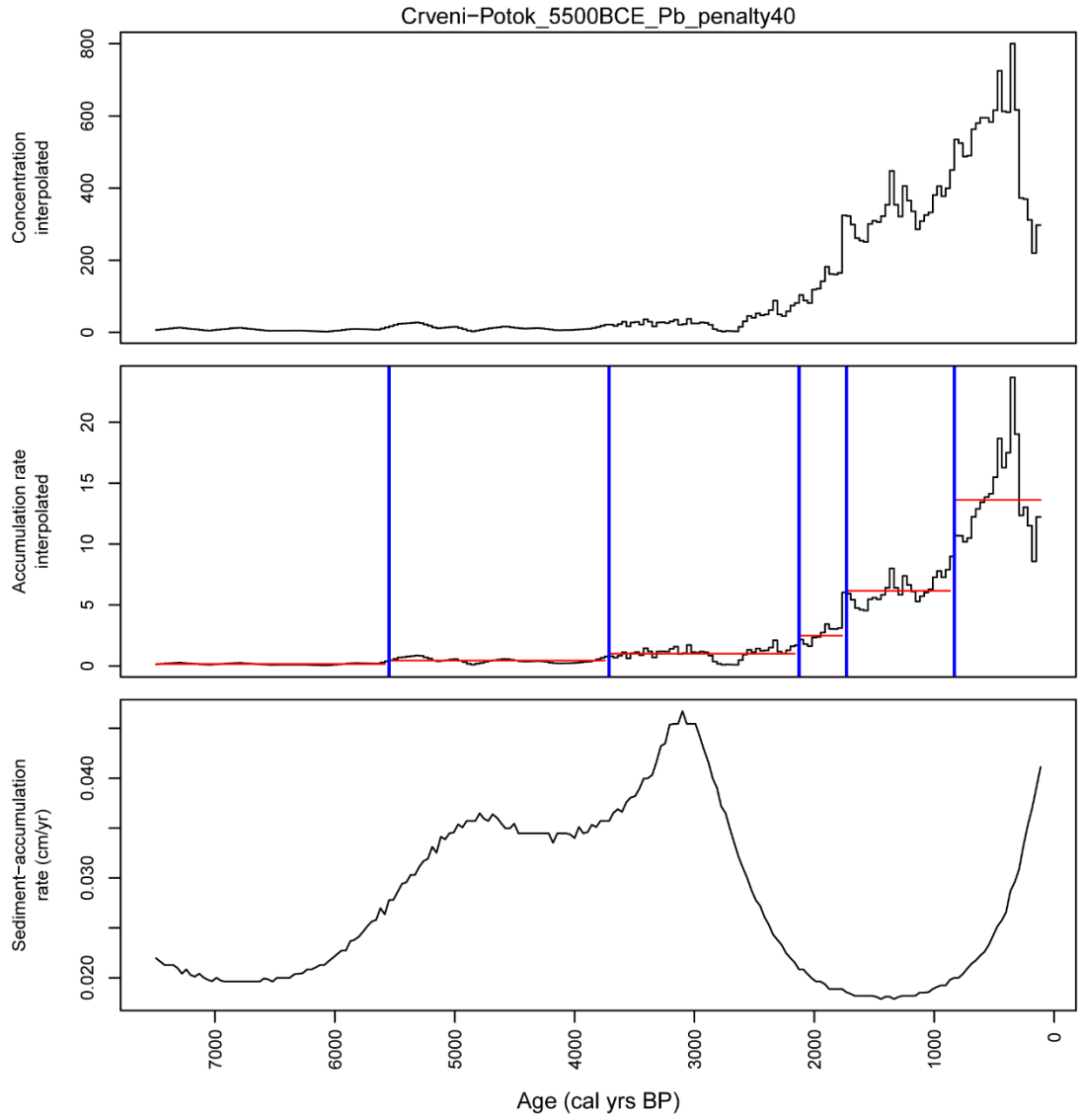

Fig. S7. Comparison between BS analysis for change-points and sediment-accumulation rates for the Pb_{Anthro} accumulation rate record of the Crveni Potok sediment sequence. Black lines in top and middle panels: interpolated Pb_{Anthro} record; vertical blue lines: change points in the measured Pb series. Under more conservative test conditions here (penalty = 40), no changepoints (empty red circles) appear in Pb records based on random Pb-concentration records (middle panel). See fig S5 for a less-conservative penalty example.

Table S1. Expected and observed recoveries for elements analyzed within Crveni Potok core. These values are derived from the analysis of certified reference materials (CRMs), of known elemental composition. Two CRMs were analyzed, NIMT/UOE/FM/001(1), a low ash peat standard, and Montana Soil 2711, a soil standard containing elevated metal contamination. Recoveries for nearly all elements are within 10% of expected values, indicating good recovery via the method utilized.

CRM 1- NIMT/UOE/FM/001

Overall Average

Element	Detection Limit (ppm)	Expected (ppm)	Average of analyzed values (ppm)	SD of analyzed values	RSD (%)	**Average %Recovery**	Analysis 1 (ppm)	Analysis 2 (ppm)	Analysis 3 (ppm)	Analysis 4 (ppm)	Analysis 5 (ppm)
Cu	0.054	5.28	5.49	0.82	14.94	**104.0**	5.86	5.01	4.16	6.52	5.9
Cr	0.006	6.36	5.32	0.47	8.87	**83.7**	4.96	5.69	5.77	4.57	5.61
Ni	0.01	4.1	4.18	0.79	18.94	**102.0**	4.2	3.31	5.41	4.62	3.36
Pb	0.042	174	177.74	12.69	7.14	**102.1**	190.41	193.13	161.08	177.83	166.34
Ti	0.0038	357	323.88	9.29	2.87	**90.7**	330.89	336.71	317.02	324.04	310.81
Zn	0.0018	28.6	27.83	1.49	5.37	**97.3**	26.19	26.06	28.27	29.93	28.69

CRM 3- Montana Soil 2711

Overall Average

Element	Detection Limit (ppm)	Expected (ppm)	Average of analyzed values (ppm)	SD of analyzed values	RSD (%)	**Average %Recovery**	Analysis 1 (ppm)	Analysis 2(ppm)	Analysis 3 (ppm)	Analysis 4 (ppm)	Analysis 5 (ppm)
Sc	0.0015	9	10.40	1.80	17.32	**115.5**	10.19	10.88	7.24	12.79	10.88
Sr	0.0004	245.3	234.48	9.92	4.23	**95.6**	250.94	225.52	229.65	225.62	240.73
Zr	0.0071	230	231.91	29.12	12.55	**100.8**	207.16	232.07	286.83	208.10	225.35

Table S2. Radiocarbon dates used to construct the age model for Crveni Potok

Lab Code	Depth (cm)	Material Dated	Sample Weight(mg)	^{14}C Age (2σ)
Poz-72891	18	*Spaghnum* stems	8.5	260±30
Poz-72892	22	36 *Picea* sp. needle pits; 1 *Abies* sp. needle pits; *Sphagnum* stems	5.2	345±30
Poz-58430	58	*Sphagnum* stems; 1 *Picea abies* Seed; 6 *Potentilla* fruits; 1 *Picea abies* Needle	11.9	2415±30
Poz-55928	93	Bark, indet.	6.1	3005±35
Poz-55929	142	Wood (Picea/Larix type)	20.5	4120±35
Poz-58431	182	Wood fragments (Larix/Picea or Pinus sp.)	5.2	5120±35
Poz-55930	218	Wood (Picea/Larix type)	13	6890±40
Poz-55931	236	Wood (Picea/Larix type)	34.9	7460±40
Poz-55932	248	Wood (Picea/Larix type)	3	7920±50

Additional data table S1 (separate file)

Pb-related analytical data from Crveni Potok core. Alongside depth, age and density, raw concentrations of Pb and Zr are presented. Calculated values for Pb enrichment factor, lithogenic contribution, anthropogenic contribution, CAAPb and Pb accumulation rate are also displayed.

Additional data table S1 (separate file)

Raw analytical data for all elements analyzed in the Crveni Potok core, including internal standard value. In addition to mean values, standard deviations and relative standard deviation values are presented.

Additional data table S1 (separate file)

Repeat data from Crveni Potok core. At seven depths, analysis was run twice on the same sample (with different subsamples). Raw results of each run, and the variation between the two measurements is presented here.

References

1. Yafa C, et al. (2004) Development of an ombrotrophic peat bog (low ash) reference material for the determination of elemental concentrations. J Environ Monit 6(5):493–501.
2. Wedepohl KH (1995) The composition of the continental crust. Geochim Cosmochim Acta 59(7):1217–1232.
3. Shotyk W, Blaser P, Grünig a., Cheburkin a. K (2000) A new approach for quantifying cumulative, anthropogenic, atmospheric lead deposition using peat cores from bogs: Pb in eight Swiss peat bog profiles. Sci Total Environ 249(1–3):281–295.
4. Weiss D, Shotyk W, Appleby PG, Kramers JD, Cheburkin AK (1999) Atmospheric Pb Deposition since the Industrial Revolution Recorded by Five Swiss Peat Profiles: Enrichment Factors, Fluxes, Isotopic Composition, and Sources. Environ Sci Technol 33(9):1340–1352.
5. Gallagher K, et al. (2011) Inference of abrupt changes in noisy geochemical records using transdimensional changepoint models. Earth Planet Sci Lett 311(1–2):182–194.
6. Kylander ME, et al. (2016) Potentials and problems of building detailed dust records using peat archives: An example from Store Mosse (the Great Bog), Sweden. Geochim Cosmochim Acta 190:156–174.
7. Scott AJ, Knott M (1974) A Cluster Analysis Method for Grouping Means in the Analysis of Variance. Biometrics 30(3):507.
8. Killick R, Eckley I (2013) changepoint: An R Package for changepoint analysis. J Stat Softw 58(3):1–15.
9. Finsinger W, et al. (2016) Holocene fire-regime changes near the treeline in the Retezat Mts. (Southern Carpathians, Romania). Quat Int. doi:10.1016/j.quaint.2016.04.029.
10. Bai J, Perron P (2003) Computation and analysis of multiple structural change models. J Appl Econom 18(1):1–22.
11. Zeileis A, Kleiber C, Krämer W, Hornik K (2003) Testing and dating of structural changes in practice. Comput Stat Data Anal 44(1–2):109–123.
12. Barry D, Hartigan JA (1993) A Bayesian Analysis for Change Point Problems. J Am Stat Assoc 88(421):309–319.
13. R Core Team T (2017) R: A language and environment for statistical computing (R Foundation for Statistical Computing, Vienna, Austria).

14. Blarquez O, et al. (2014) paleofire: An R package to analyse sedimentary charcoal records from the Global Charcoal Database to reconstruct past biomass burning. Comput Geosci 72:255–261.
15. Higuera PE, Brubaker LB, Anderson PM, Hu FS, Brown TA (2009) Vegetation mediated the impacts of postglacial climate change on fire regimes in the south-central Brooks Range, Alaska. Ecol Monogr 79(2):201–219.
16. Erdman C, Emerson JW (2007) bcp : An R Package for Performing a Bayesian Analysis of Change Point Problems. J Stat Softw 23(3). doi:10.18637/jss.v023.i03.
17. Zeileis A, Leisch F, Hornik K, Kleiber C (2002) strucchange: an R package for testing for structural change in linear regression models. J Stat Softw 7(2):1–38.
18. Lazarević PM (2013) Mires of Serbia - Distribution characteristics. Bot Serbica 37(1):39–48.
19. Shotyk W, Krachler M, Martinez-Cortizas A, Cheburkin AK, Emons H (2002) A peat bog record of natural, pre-anthropogenic enrichments of trace elements in atmospheric aerosols since 12 370 14C yr BP, and their variation with Holocene climate change. Earth Planet Sci Lett 199(1–2):21–37.
20. De Vleeschouwer F, et al. (2009) Multiproxy evidence of `Little Ice Age' palaeoenvironmental changes in a peat bog from northern Poland. The Holocene 19(4):625–637.
21. Finsinger W, et al. (2017) Holocene vegetation and fire dynamics at Crveni Potok, a small mire in the Dinaric Alps (Tara National Park, Serbia). Quat Sci Rev 167:63–77.
22. Marković SB, et al. (2015) Danube loess stratigraphy — Towards a pan-European loess stratigraphic model. Earth-Science Rev 148:228–258.
23. Shotyk W (2002) The chronology of anthropogenic, atmospheric Pb deposition recorded by peat cores in three minerogenic peat deposits from Switzerland. Sci Total Environ 292:19–31.
24. Monna F, et al. (2004) Environmental impact of early Basque mining and smelting recorded in a high ash minerogenic peat deposit. Sci Total Environ 327(1–3):197–214.
25. Longman J, Ersek V, Veres D, Salzmann U (2017) Detrital events and hydroclimate variability in the Romanian Carpathians during the Mid-to-Late Holocene. Quat Sci Rev 167:78–95.